# Pilot Field Implementation of Suction Dredging for Sustainable Sediment Management of Dam Reservoirs

Sameh A. Kantoush, M.ASCE[1]; Ahmad Mousa[2]; Ebi Meshkati Shahmirzadi[3]; Temmyo Toshiyuki[4]; and Tetsuya Sumi[5]

**Abstract:** The buildup of sediment deposits in reservoirs is a long-standing problem with serious consequences on the reservoirs' functionality and the ecology of their river systems. In the last two decades, hydraulic dredging has been used as a more viable engineering solution to restore reservoirs' sustainability. This study proposes a novel ejector-pump dredging system (EPDS) that solely utilizes hydraulic dredging for removal and transport of the sediments deposited at the reservoir's bed. Unlike conventional dredging methods, air is injected into the header pipeline to create a turbulent three-phase flow regime that enhances the solids suspension and continuous flow in the system. Introducing air effectively reduces the critical value of the deposition velocity of the dredged solids and transports them in a slug flow regime. This technique minimizes the tendency of the sediment to settle, and therefore eliminates system plugging. A laboratory prototype of the proposed system has proven the efficacy of removal and transport of mixed-size sediments up to 150 mm. Field trials have further shown the feasibility of the proposed system. Removal of large sediments with productivity approaching 70 $m^3/h$ was made possible using the suction-type EPDS. The hopper-type EPDS enabled carrying the dredged material for up to 1,000 m without resorting to a booster pump. The developed system was successfully used as part of an integrated dredging management program carried out for the Oouchibaru, Saigo, and Yamasubaru dams in the Mimi River basin, Japan. The very low turbidity levels recorded during the sediment dredging and transport operations of EPDS are indicative of the eco-friendly performance of the system. **DOI:** 10.1061/(ASCE)HY.1943-7900.0001843. 

**Author keywords:** Sediment management; Suction dredging; Dam reservoir; Three-phase flow; Ejector-pump dredging system (EPDS); Turbidity control.



## Introduction

Sediment management in dam reservoirs has become an increasingly inevitable priority for management boards of river basins worldwide. The recurrence of excessive siltation upstream of dam reservoirs not only leads to costly reservoir storage maintenance, it also imbalances the sediment inflow and outflow in the reservoirs, which may result in dire consequences on a river's ecosystem (Morris 2020; Kantoush and Sumi 2019). A range of sediment management techniques, such as flushing, sediment bypass tunnel, sluicing, and dredging, has been developed to restore dams' functionality and recover their ecosystem (Auel et al. 2016). Selecting one or a combination of these techniques is site specific and mainly depends on the turnover rate of both water and sediments (Kantoush and Sumi 2016). The factors governing the selection include the type and amount of sediments, dredging depth, distance to the disposal site, and operating conditions (Basson and Rooseboom 1999; Chaudhuri et al. 2020; Bray et al. 1996).

Hydraulic dredgers utilize water to break and lift sediments and transport them to a designated disposal site (Turner 1996; Herbich 2000). They are capable of removing a wide array of materials, e.g., clay, mud, silt, sand, gravel, and reef material (Morris 2020; Lewis and Randall 2015). Hydraulic dredgers include trailing suction hopper dredger (TSHD), bucket wheel, plain suction or dustpan, and cutter-suction dredger (CSD). Siphon dredging and the sediment evacuation pipeline system are differentiated from other hydraulic dredgers by the absence of a pump and a continuously submerged discharge (Morris 2020). Conventional hydraulic dredging systems have limited transportation lengths and require a lot of power to restore the storage capacity of a reservoir (Bruk 1985). They are typically challenged by the frequent deposition of the dredged material in the transport pipeline (TP), especially for long distances. This could lead to serious subsequent problems, such as excessive pressure drops, equipment failure, and pipeline erosion, all of which adversely affect dredging productivity (Chaudhuri et al. 2020).

The presence of two- or three-phase flow (water, sediment, and air) in a transport pipeline can form different slurry flow regimes (Herbich 2000): homogeneous, heterogeneous, moving bed, and stationary bed. Mandhane et al. (1974) conducted two-phase air and water flow tests to monitor the flow regimes of water–air mixtures in a horizontal pipe. They found that the flow patterns depend largely on the influx combinations of water and air. In terms of pattern, there are six key flow regimes, namely, dispersed bubble, annular, elongated bubble, slug, stratified, and stratified wavy flow (Taitel and Dukler 1976). Three-phase flows (air–water–sand)

[1]Associate Professor, Disaster Prevention Research Institute, Kyoto Univ., Ujishi Gokasho Kyoto 611-0011, Japan. ORCID: https://orcid.org/0000-0003-0919-5097. Email: kantoush.samehahmed.2n@kyoto-u.ac.jp

[2]Senior Lecturer, School of Engineering, Monash Univ. Malaysia, Selangor 46150, Malaysia (corresponding author). ORCID: https://orcid.org/0000-0002-6057-3885. Email: ahmad.mousa@monash.edu

[3]Engineer, Researcher, Deltares, Boussinesqweg 1, 2629 HV Delft 2629, Netherlands. Email: ebi.meshkatishahmirzadi@deltares.nl

[4]Engineer, International Div., Hazama Ando Corporation, 6120 Akasaka Minatoku, Tokyo 107-8658, Japan. Email: temmyo.toshiyuki@ad-hzm.co.jp

[5]Professor, Disaster Prevention Research Institute, Kyoto Univ., Ujishi Gokasho Kyoto 611-0011, Japan. Email: sumi.tetsuya.2s@kyoto-u.ac.jp

Note. This manuscript was submitted on September 20, 2019; approved on August 31, 2020; published online on December 4, 2020. Discussion period open until May 4, 2021; separate discussions must be submitted for individual papers. This paper is part of the ***Journal of Hydraulic Engineering***, © ASCE, ISSN 0733-9429.

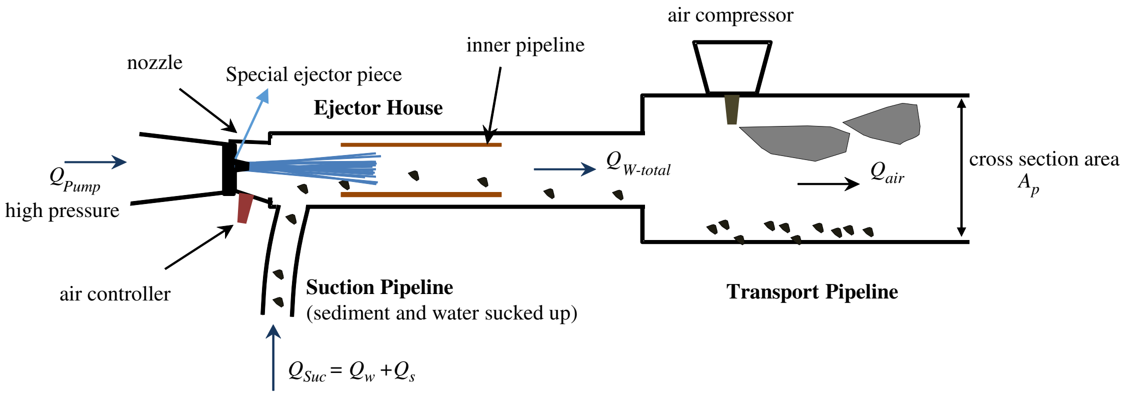


**Fig. 1.** Concept of the ejector house (EPDS).

in a horizontal pipe have been closely investigated in both experimental and numerical studies using different air concentrations (e.g., Goharzadeh et al. 2010; Dabirian et al. 2016a, b; Leporini et al. 2018). The existing studies are mainly devoted to applications in the petroleum industry at laboratory scale. This study, however, investigates multiphase flow sediment transport tailored to dredging application at both the laboratory and commercial scale, with a focus on the impact of air injection on the efficiency of the dredging system as a whole. This study was motivated by the growing demand for dredging to restore the storage capacity of several dam reservoirs in Japan. The restoration requirements span efficient, economical, reliable, and environmentally accepted dredging. Reservoir dredging is being carried out for a quarter of the 3,000 dams in Japan. We propose a novel hydro-suction dredging technique that chiefly employs suction for sediment removal. The air injection creates a multiphase flow (water–air–solid) that can optimize the suction power and equally minimize plugging in the transportation components. The adopted concept has proven to be successful both at the laboratory scale and in the field trials in Morotsuka, Yamasubaru, Saigo, and Ouchibaru reservoirs in Japan. The implementation includes sediment relocation within the reservoirs as well as transporting the removed dredged sediment to designated disposal areas.

## Laboratory Prototype

A laboratory prototype utilizing forced hydro-suction for sediment removal was built as a proof of the concept. Experimental evaluation of the system establishes a fundamental understanding of the system's performance and examines its sensitivity to the design parameters. The mechanism and efficiency of the sediment suction and transport were closely monitored for system optimization.

### *Operating Concept*

The proposed ejector-pump dredging system (EPDS) employs a high-pressure water jet applied through a nozzle to create negative pressure in the ejector house. The ejector subsequently delivers the necessary energy to draw the sediment from the reservoir bed through a vertical suction pipeline (Fig. 1). The sediments entering the ejector house are pushed into the transport pipeline under the high-pressure water jet. The ejector pump has two specific characteristics: a controlled air inlet into the pump; and the unthrottled inner straight pipe (Fig. 1). This configuration minimizes cavitation and abrasion of the pump. By changing a combination of diameters of the nozzle and the inner pipe, the suction flow rate can be adjusted. Another advantage is that the jet flow washes the sediment while passing through the ejector pump. Because the new pump does not have rotary parts (impeller wheel), it is structurally simple and easy to maintain.

As schematically shown in Fig. 2, the experimental setup consists of three major sections, namely, the initial driving force, suction, and transport. The driving force section comprises a high-pressure pump connected to a storage tank. This component of the setup generates a high-velocity water jet responsible for creating negative pressure (suction) in the ejector. Suction from the sediments tank is furnished via a vertical pipeline having an internal diameter ($D_{sp}$). Several pipe lengths ($H_{suc}$) were considered in this setup (Table 1). Transport of the drawn sediments was made possible through a horizontal pipeline ($L_{tp}$, $D_{tp}$) running from the air compressor injection point to the downstream end (disposal). The compressor injects a controlled air concentration at the head of the transport pipeline. A 1-m segment of the horizontal transport pipe was made of transparent plexiglass to permit flow visualization using the large-scale particle image velocimetry (LSPIV) technique. The system is equipped with two static-dynamic pressure gauges ($P1$ and $P2$) at the high-pressure pump and downstream of the ejector house, respectively. Three pressure probes/piezometers ($P3$, $P4$, and $P5$, located 3.5 m apart) are used to measure the pressure differential in the transport pipeline. To this end, the designed experimental program aims to utilize the collected observations to identify the key factors and parameters that control suction dredging. Subsequently, the system was optimized to enhance efficiency and minimize clogging potential.

### *Design Parameters*

The suction power ($Q_{suc}$) from a sediment tank is defined as the volume of water and sediment lifted during a specific time period. Several inherent properties of the flow mix, namely, the densities of water ($\rho_w$) and sediments ($\rho_s$), and the grain size ($d_s$) affect the suction power. It is also governed by other parameters including the pump discharge pressure ($P_{\text{pump}}$), air concentration ($Q_{\text{air}}$) injected to the pipeline, length of the suction pipeline ($L_{sp}$), length of the transport pipeline ($L_{tp}$), height of the suction pipeline ($H_{sp}$), diameter of the suction pipeline ($D_{sp}$), and diameter of the transport pipeline ($D_{tp}$). As such, the suction flow can be expressed as a function of these parameters

$$Q_{suc} = f(d_s, P_{\text{pump}}, Q_{\text{air}}, L_{tp}, H_{sp}, D_{\text{sp}}, D_{\text{tp}}, \rho_w, \rho_s) \qquad (1)$$

The experiments were carried out for five sediment grain sizes, five pump discharges, eight air concentration levels, four lengths of suction pipe, seven lengths of transportation pipeline, and five





J. Hydraul. Eng., 2021, 147(2): 04020098

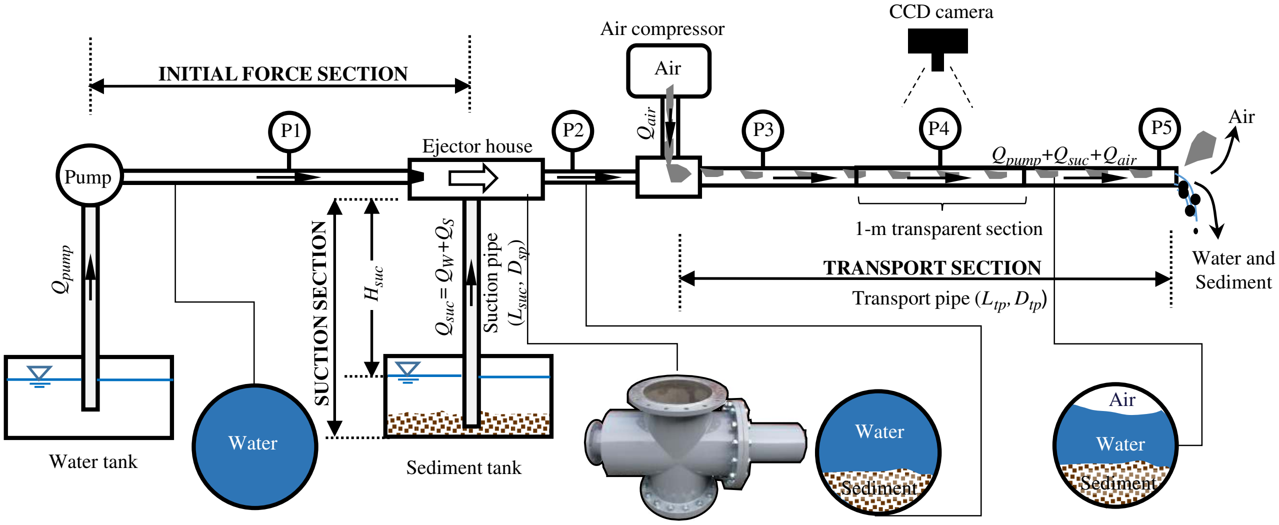


**Fig. 2.** Laboratory EPDS prototype.

suction heads. The laboratory program amounts to a total of 215 experiments, as summarized in Table 1. Two liters of sediments ($V_s$) were placed in the sediment storage tank. The time needed for suction and removal of the sediments at the end of the transport pipe was recorded ($t_{ws}$) for each test. Thus, the sediment discharge rate ($Q_s$) can be calculated as

$$Q_s = V_s/t_{ws} \tag{2}$$

The difference between the water level in the sediment tank before and after the test yields the released volume of water and sediments ($V_{ws}$). The suction power ($Q_{suc}$) can be accordingly estimated as

$$Q_{suc} = V_{ws}/t_{ws} \tag{3}$$

The superficial velocities $J_A$ and $J_W$ are respectively defined as the air concentration ($Q_{\text{air}}$) and water-sediment flow discharge ($Q_{ws}$) passing through the pipeline cross-sectional area ($A_p$). In the pipeline, $Q_{ws}$ is the sum of the pump discharge ($Q_{\text{pump}}$) and the water-sediment mix sucked from the sediment reservoir ($Q_{suc}$). The superficial velocities of the flow in the pipeline can be subsequently expressed as follows:

$$J_A = Q_{\text{air}}/A_p \text{ (air)} \tag{4}$$

$$J_W = Q_{(W-\text{total})}/A_p \text{ (water} - \text{sediment)} \tag{5}$$

$$J = J_A + J_W \text{ (total)} \tag{6}$$

The overall efficiency ($E_{\text{EPDS}}$) of the system performance can be defined as the ratio between the sediment and the pump discharges

$$E_{\text{EPDS}} = Q_s/Q_{\text{pump}} \tag{7}$$

Both $Q_{suc}$ and $E_{\text{EPDS}}$ are practical indicators of the performance. They can subsequently provide reasonable guidance for system design and optimization. However, they are likely to be influenced by sediment size ($d_s$), geometry of the prototype ($D_{sp}$, $D_{tp}$, $L_{sp}$, $L_{tp}$), and the hydraulic parameters ($Q_{\text{air}}$, $H_{suc}$). Sediment removal concentrations in the suction pipeline ($C_{ss}$) and transport ($C_{st}$) phases are respectively expressed as follows:

$$C_{ss} = Q_s/(Q_s + Q_w) \times 100 \tag{8}$$

$$C_{st} = Q_s/(Q_{\text{pump}} + Q_s + Q_w) \times 100 \tag{9}$$

Eqs. (8) and (9) provide additional practical measures for the efficiency of sediment removal in the suction and transport pipelines, respectively.

## Results

The laboratory program monitored the flow regimes using the proposed system and evaluated the efficiency of the suction and transport phases. Table 1 summarizes the investigated ranges of the key design parameters. The values of $D_{sp}$ and $D_{tp}$ were set at 25 and 36 mm, respectively, for all of the presented laboratory readings. In any given trial, $\rho_s$, $H_{suc}$, $L_{sp}$, and $L_{tp}$ were held constant unless stated otherwise. As such, the interaction between the selected parameters and the laboratory measurements should not be overruled.

### Flow Regimes

The observed air and water superficial velocities at air injections of up to 120 nL/min were as follows:

$$0.409 < J_A < 1.96 \text{ m/s}$$

$$0.411 < J_W < 1.52 \text{ m/s}$$

**Table 1.** Geometrical and hydraulic parameters for laboratory investigation

| Parameter | Range and value |
|---|---|
| $d_s$ (mm) | 0 (clear), 2, 5, 10, 15 (large), mixed (1:1 bulk volume of 2 and 5 mm) |
| $P_{\text{pump}}$ (kPa) | 196, 294, 490, 588, 687 |
| $Q_{\text{air}}$ (nL/min) | 0, 25, 40, 50, 60, 80, 100, 120 |
| $L_{sp}$ (m) | 1, 3, 10, 20 |
| $L_{tp}$ (m) | 1, 5, 7, 10, 15, 20, 30 |
| $D_{sp}$ (mm) | 25 |
| $D_{tp}$ (mm) | 36 |
| $H_{suc}$ (m) | 0.2, 1.2, 0.5, 1.5, 2.5 |



J. Hydraul. Eng., 2021, 147(2): 04020098

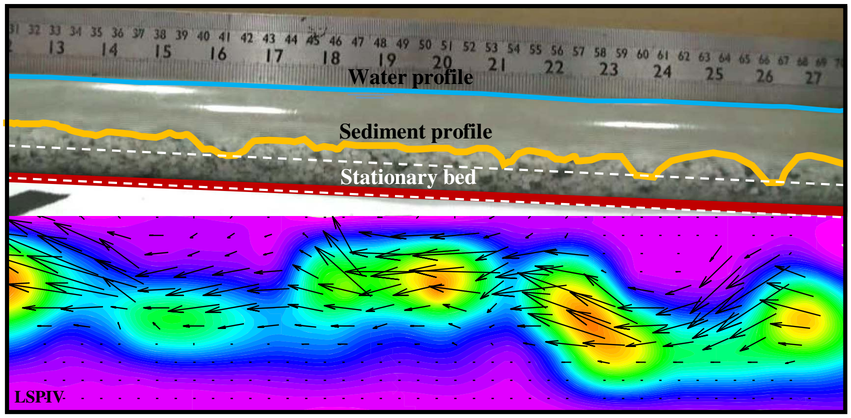


(a)

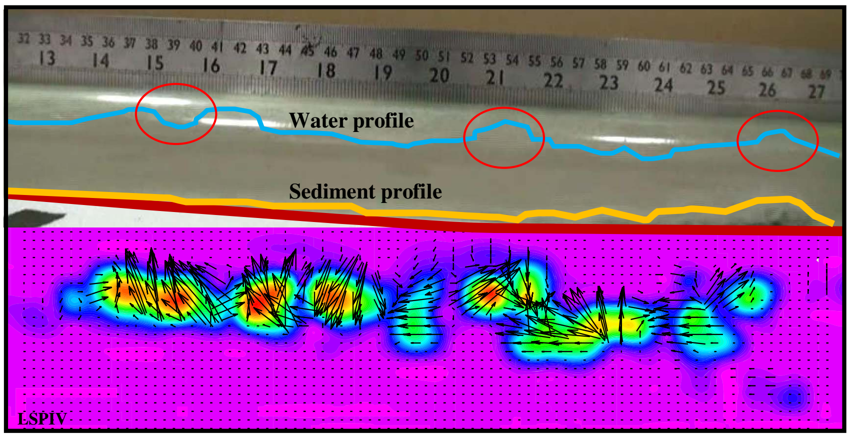


(b)

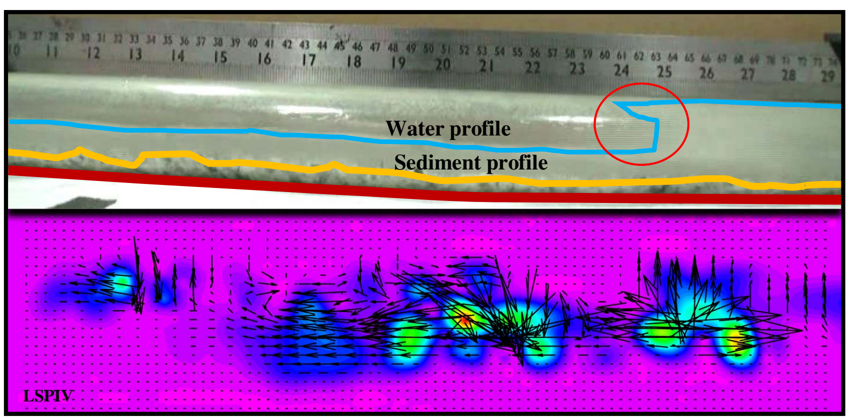


(c)

**Fig. 3.** Flow profile and PIV average distribution in a straight segment of transport pipe ($d_s = 2$ mm, $P_{\text{pump}} = 0.196$ MPa) for (a) $Q_{\text{air}} = 0$ nL/min; (b) $Q_{\text{air}} = 25$ nL/min; and (c) $Q_{\text{air}} = 40$ nL/min (top grading on ruler is in centimeters).

The ranges for the collected velocities are overlain on the flow-type zones depicted in Fig. S1. The flow patterns associated with these ranges are clearly slug-plug types. When the flow regime changes from elongated bubble flow to slug at the minimum superficial air velocity of 0.95 m/s, the velocity at this transition state cannot be determined with certainty. Hence, the flow pattern should be closely monitored to provide a qualitative measure of the particle movement regime. Interactions of solid–gas–liquid in a multiphase flow and flow field analysis have been investigated using the particle image velocimetry (PIV) technique (Kim et al. 2018). In this study, LSPIV analysis was employed to visualize the flow pattern in the transport phase (Kantoush et al. 2011).

Fig. 3(a) depicts the captured flow along with the velocity distribution in a TP when no air was injected into the system. This was manifested in forming a stratified flow in the pipe. Almost all velocity vectors are confined in the upper half of TP with a general horizontal flow. The flow vectors in the sediment deposits are insignificant. This indicates the inability of the stratified flow to carry the sediments. However, when 25 nL/min airflow was injected into the system, the velocity distribution significantly changed [Fig. 3(b)].

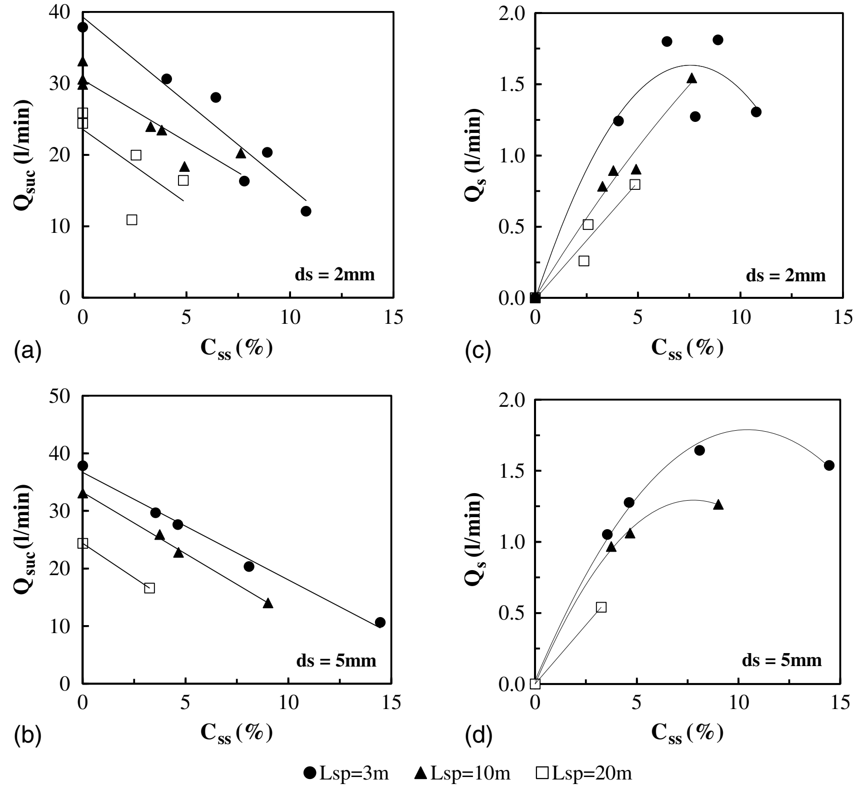


**Fig. 4.** Sediment removal in the suction section ($C_{ss}$) for 2- and 5-mm particles: (a and b) $Q_{suc}$; and (c and d) $Q_s$ ($P_{\text{pump}} = 588$ kPa, $Q_{\text{air}} = 0$ nL/min).

As shown by the traced trajectories, an intermittent flow pattern was observed and the velocity vectors are periodically oriented toward the bottom of TP. The efficiency of particle stirring and suspension was increased when the airflow was raised to 40 nL/min [Fig. 3(c)].

## Suction Phase

As discussed previously, the applied high jet velocity drops the pressure in the ejector house and thus enables the system to vacuum (suck) sediments from the reservoir via a suction pipeline utilizing the created pressure gradient. The wide range of discharge pump pressures ($P_{\text{pump}}$) and various sizes of sediments used in this study [previously reported by Meshkati Shahmirzadi et al. (2012)] allowed correlation with the suction power ($Q_{suc}$) at different air concentrations. At higher $P_{\text{pump}}$, the jet velocity of the water released from the nozzle greatly increases and causes a high pressure drop (negative pressure) in the ejector house. The created pressure gradient between the sediment tank and the ejector house subsequently lifts the water and sediments ($Q_{suc}$) into the EPDS header. As expected, $Q_{suc}$ in the presence of only clear water was higher than that of the two-phase (sediment-water) flow.

Further pressure gradient can be achieved by injecting air downstream of the ejector house. This additional pressure differential is created between the beginning of the transport pipeline (just downstream of the ejector house) and the inside of the inner pipe in the ejector house. Air injection increases the velocity of flow, i.e., $J_A$ and $J_W$, and thus the velocity at the beginning of transport pipeline should be higher than that inside of the inner pipe in the ejector house. The induced dual vacuum effect enhances sediment transport with higher initial velocities compared to the zero-air injection. This reduces the risk of sediment accumulation in the beginning of the pipeline and improves the efficiency of sediment transport.

The effect of the suction pipe length on flow of dredged water and sediment was tested. Fig. 4 depicts the sediment concentration in the suction pipe ($C_{ss}$) compared with $Q_{suc}$ and $Q_s$ for the 2- and 5-mm sediments. The results are shown for zero-air entrainment and pumping power ($P_{\text{pump}}$) of 588 kPa. Increasing the suction power $Q_{suc}$ was associated with a linear reduction in concentration of sediment in the suction pipe, $C_{ss}$. This was observed for sediment sizes of 2 and 5 mm and for all lengths of the suction pipe [Figs. 4(a and b)]. Moreover, for a certain $C_{ss}$, the shorter the length of suction pipe, the larger the suction power of the system $Q_{suc}$. This does not mean that more sediment will be removed. As can be seen in Figs. 4(c and d), there is an optimal value for $C_{\text{ss}}$ in the shortest suction pipe (2 m) at which the maximum sediment discharge rate $Q_s$ occurs. Thus, the maximum sediment removal performance does not occur at the highest $C_{ss}$. For longer suction pipes (10 and 20 m), however, it was not possible to increase the $C_{\text{ss}}$ beyond a certain concentration because the system failed at those higher concentrations. Fig. 5 shows the maximum observed sediment discharge rate $Q_s$ for the three suction lengths in the presence of no air injection in the transport pipe. As expected, for a certain suction pipe length, the smaller the particles, the better the performance of system regarding sediment discharge rate ($Q_s$).

## Transport Phase

The differential pressure in the transport pipeline was monitored using the piezometers shown in Fig. 2. The pressure gradient ($\delta p/\delta x$) was calculated as the pressure difference between P3 and P5 divided by the distance ($\Delta x$) between piezometers



J. Hydraul. Eng., 2021, 147(2): 04020098

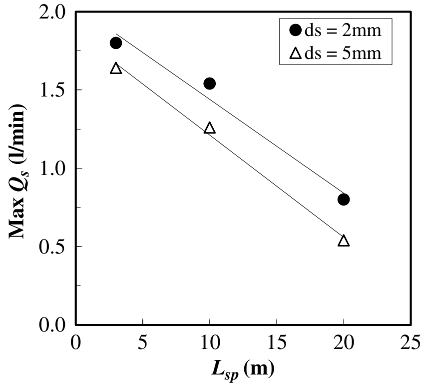


**Fig. 5.** Maximum sediment discharge ($Q_s$) for different suction pipe lengths ($P_{\mathrm{pump}} = 588$ kPa, $Q_{\mathrm{air}} = 0$ nL/min).

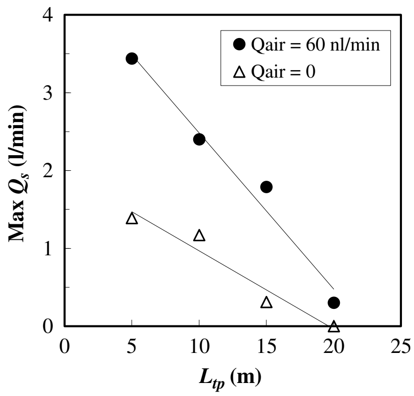


**Fig. 6.** Maximum sediment discharge ($Q_s$) for different transport pipe lengths ($P_{\mathrm{pump}} = 588$ kPa, $d_s = 5$ mm).

$$\delta p/\delta x = (\mathrm{P3} - \mathrm{P5})/(\Delta x) \tag{10}$$

The sediment removal in suction ($C_{ss}$) and the measured sediment concentration in the transport pipe ($C_{st}$) (Fig. S2) have improved by using air injection particularly for the larger sediment (5 mm). These relationship between both $C_{ss}$ and $C_{st}$ and the observed pressure gradient advocates that the change in the flow pattern due to air injection enhances the suction and transport processes (Meshkati Shahmirzadi et al. 2012). The relation between the length of the transport pipeline and the maximum observed sediment discharge rate ($Q_s$) is shown in Fig. 6. The maximum $Q_s$ decreases linearly with increasing the transport length. The use of 60 nL/min air injection resulted in higher $Q_s$ compared to the zero-air case. The presence of air in the transportation managed to increase the sediment removal even for the near-zero removal at $L_{tp}$ of 20 m. This result suggests the need to optimize the air concentration for long transportation, which could be extremely beneficial in the field.

### *System Optimization*

The foregoing results provided the basis for optimization of the geometrical and hydraulic characteristics of the system. In doing so, the efficiency and the performance of the system are quantified. The concentration of the injected air is the key factor in the system optimization. Different sediment sizes and suction powers were used for this purpose.

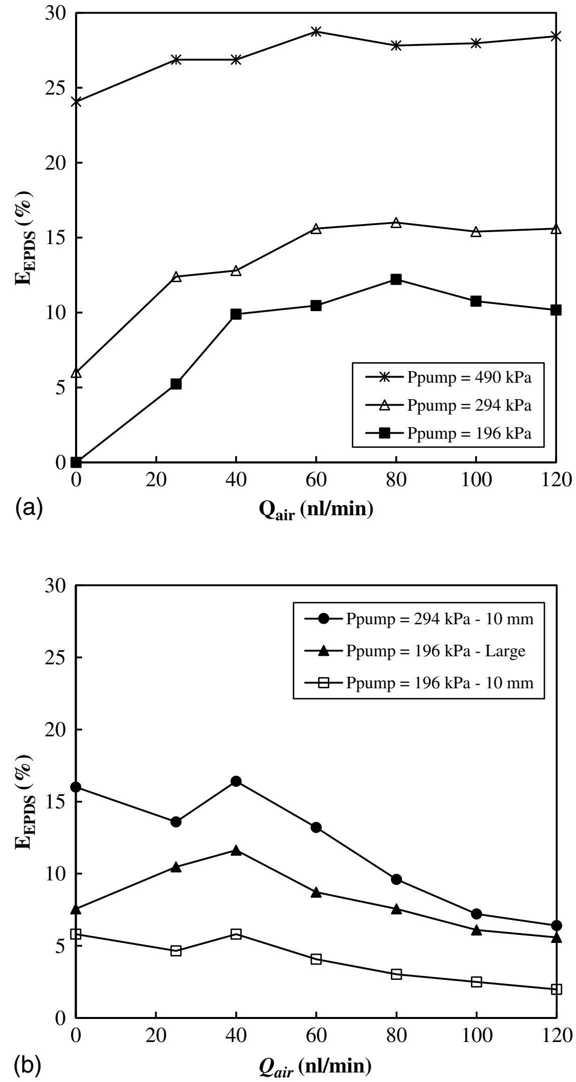


**Fig. 7.** Effect of air concentration ($Q_{\mathrm{air}}$) on the overall efficiency of the system ($E_{\mathrm{EPDS}}$) using different suction powers ($P_{\mathrm{pump}}$): (a) $d_s = 2$ mm; and (b) $d_s = 10$ and 15 mm (large).

Fig. 7 depicts the relationships between the overall efficiency of the system ($E_{\mathrm{EPDS}}$) and air concentration ($Q_{\mathrm{air}}$) for fine (2 mm), medium (5 mm), coarse (10 mm), large (15 mm), and mixed particles using different pump pressures. The mixed particles are nonuniform mixtures of equal volume proportions of 2- and 5-mm grains (i.e., 1:1 bulk volume). As shown in Fig. 7(a), increasing $Q_{\mathrm{air}}$ was associated with a continuous improvement in efficiency for the 2-mm sediments. The overall efficiency of the system in removal of medium and large (15-mm) sediments exhibited some fluctuation over the same range of air injections [Fig. 7(b)]. For these sediments there seems to be an optimum air concentration range for the highest observed $E_{\mathrm{EPDS}}$. Indeed, the higher $Q_{\mathrm{air}}$ intensified the suspension of fine sediments into the slug flow body, allowing them to be carried a longer distance in the slug flow. The dredging system exhibited its best performance when an intermediate concentration of air between 40 and 80 nL/min was used.

The total superficial velocity ($J$) and efficiency ($E_{\mathrm{EPDS}}$) were calculated for 11 selected cases (different sediment sizes and pump pressures) using a range of air concentrations. It was found that raising the air concentration increased $J$ values for all cases [Fig. 8(a)], but not necessarily $E_{\mathrm{EPDS}}$ [Fig. 8(b)]. More specifically,

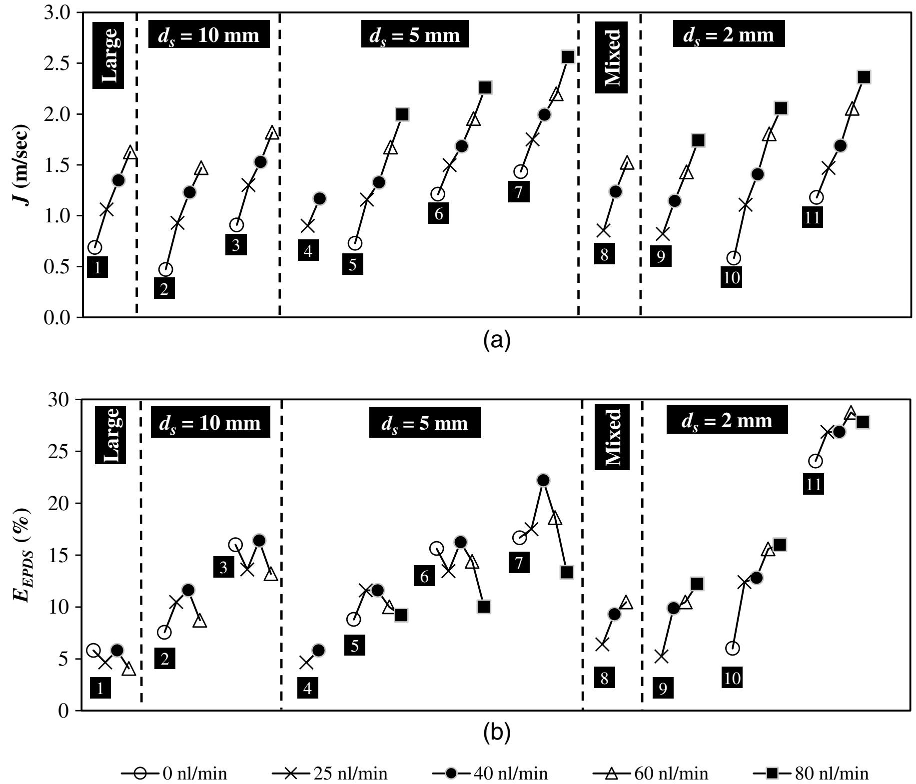


**Fig. 8.** Effect of air injection ($Q_{\mathrm{air}}$) on (a) total superficial velocity of the flow ($J$); and (b) overall system efficiency ($E_{\mathrm{EPDS}} = Q_s/Q_{\mathrm{pump}}$) [$P_{\mathrm{pump}} = 588$ kPa; Mixed is nonuniform mixtures of equal volume proportions of 2- and 5-mm grains (i.e., 1:1 bulk volume); Large is 15 mm].

increasing $Q_{\mathrm{air}}$ for large- and medium-size sediments (Cases 1–7) was not consistently associated with a corresponding increase in $E_{\mathrm{EPDS}}$, contrary to finer sediments (Cases 8–11). This is attributed to their distinct transport pattern in EPDS. As compared to large sediments, the success in boosting the efficiency of medium-size sediments is more dependent on the air concentration. The relation between the injected air into the transport pipeline and the maximum $Q_s$ is shown in Fig. 9. The maximum $Q_s$ increased with increasing $Q_{\mathrm{air}}$ up to approximately 60 nL/min, then decreased with further increase in air injection. The maximum observed $Q_s$ for 2-mm sediments is higher than that of 5-mm particles. In both cases, there seems to be an optimum air injection between 40 and 80 nL/min.

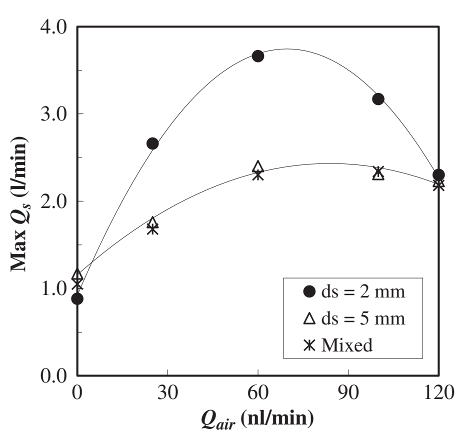


**Fig. 9.** Maximum sediment discharge ($Q_s$) for a transport pipe length of 10 m [$P_{\mathrm{pump}} = 588$ kPa; Mixed is nonuniform mixtures of equal volume proportions of 2- and 5-mm grains (i.e., 1:1 bulk volume)].

## Synopsis

The proposed system provides a number of solutions and advantages over traditional suction dredging systems. The use of a high-pressure water jet in lieu of a blade-rotary pump for generating a negative pressure (suction) allows unsupported removal of sediments. The ejector pump is less likely to jam, rust, or break down because of the absence of wings (impellers). Injection of air has proven to be instrumental for ensuring continuous dredging and minimizing system plugging commonly observed in other suction dredging systems.

Air injection forms a slug flow regime, which consequently keeps the sediments in suspension, creating the most economical sediment transportation. The air bubbles have dual roles. First, they cluster in the upper part of the pipeline, which reduces the effective cross section available to flow, and hence increases flow velocity at the same pumping capacity. Second, they are likely to be absorbed or entrapped between the sediment particles. This allows a range of positive consequences: reduction of the sediment density enhances resuspension in the system, and reduction of the settling velocity for particles already suspended in the wavy flow. Hence, sediments can be transported for a long distance by the created wave.

The experimental observations have shown that the removal mechanisms for coarse and fine sediments in EPDS are different, particularly at low pump discharge pressures. When no air is introduced in the TP, fine sediments tend to form dunes along the transport pipeline, whereas coarse sediments are transported more

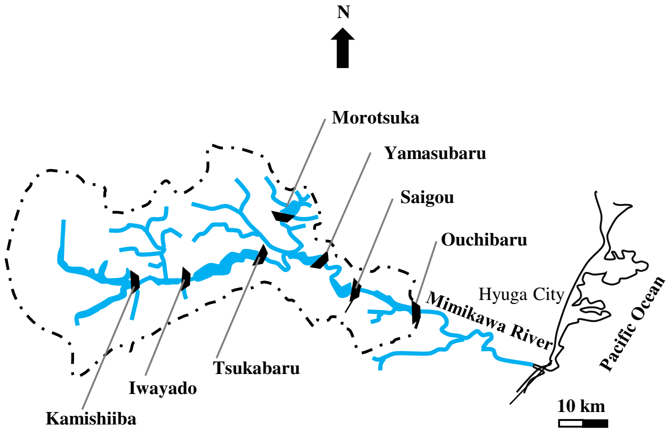


**Fig. 10.** Location of dams along Mimi River basin.

individually. Coarse particles exhibit friction against the flow and can be hardly suspended in the slug flow body. This explains their lower removal rate compared to fine sediments. On the other hand, the clustering of fine sediments (cloudlike) creates higher resistance to the flow and consequently greater pressure gradient. Therefore, the risk of pipeline blockage in the absence of air injection in TP is higher for fine sediments compared to that of the coarser sediments.

## Field Implementation

The field trials of EPDS were mainly performed at the reservoirs of the Mimi River located in Miyazaki Prefecture, southeast of Kyushu, Japan. The trials included suction dredging in Saigo, Morotsuka, and Yamasubaru reservoirs, sediment transport and gravel capping in Oouchibaru reservoir, and sediment relocation in Yamasubaru reservoir. The Mimi River has a total length of 94.8 km and a watershed area of 884.1 $km^2$. Dams in the Mimi River basin have undergone upgrading and retrofitting post-Typhoon Nabi in 2005 to increase flow and sediment release (Kantoush and Sumi 2016). Fig. 10 depicts the location of the hydropower dams and reservoirs considered in the field trials (Yamagami 2012; Nakamura et al. 2012).

The results of the laboratory phase provided a solid proof of concept to build two full-scale EPDS setups for sediment removal and relocation. The suction-type EPDS is used to remove the deposited sediments from the bottom of a reservoir and transport them to the downstream area, while the hopper-type EPDS can be used to relocate collected or stored sediments to a desired disposal site.


**Fig. 11.** Field EPDS dredging system: (a) dredging ship; (b) suction system; and (c) distributor. (Images by Temmyo Toshiyuki.)

The following section provides a description of the full-scale EPDS components and configurations.

### System Components

The main components of the field EPDS system are a high-pressure pump, ejector pump, air compressor, transport pipeline, and distributing shipboard [Fig. 11(a)]. The high-pressure pump and air compressor were set to inject 1–3 water units and 0–1 air units, respectively, into the system (1 unit is 18 $m^3/min$). The ejector house is designed to serve dual functions. First, it sucks the sediments from the bottom of the reservoir and transports them to the downstream area (suction EPDS). Second, it transports the collected sediments to a disposal area without suction (hopper EPDS). The driving force of the system from the high-pressure pump to the ejector pump is shown in Fig. 11(b). The distributing shipboard is set at the end of the transport pipeline to release the sediments [Fig. 11(c)]. The distributor is used to keep the transport pipeline on the water surface using several sets of float tubes attached to the pipe segments. Silt fences were installed to a depth of 5 m below the water surface to minimize turbidity and water pollution during sediment dredging and deposition [Fig. 11(c)].

### System Configurations and Parameters

The suction EPDS is equipped with a 220-kW pressure pump that discharges a high-velocity water jet into the ejector house through a nozzle to create negative pressure (suction). At a flow rate of approximately 5 $m^3/min$, the pump creates an equivalent suction pressure of 1.95 MPa. As shown in Fig. S3, the hopper-type EPDS assembly mounted on the shipboard hosts a conveyor belt that feeds the dredged (or stored) sediments for disposal through a hopper attached to the ejector. The sucked or stored (after dredging) sediments are subsequently discharged to a designated sediment tank. The ejector is equipped with an air controller inlet and a straight inner pipeline to eliminate cavitation as well as abrasion of the system. The air inlet valve (detail A in Fig. S3) has three settings: closed, half open, and fully open. The transport line consists of 6-m-long 400-mm PVC pipe segments connected to each other by 1-m-long rubber links for flexibility [Fig. 11(a)]. The system parameters and measuring devices are shown in Fig. S3 (also included in the notations).

### Sediment Removal

In the case of Morotsuka reservoir, dredging was performed in 4- to 9-m-deep water using 5-, 10-, 15-, and 20-m-long suction pipes. Yamasubaru reservoir was dredged by lowering the EPDS under the water surface.

Various configurations of these EPDSs, such as water pressure of the jet pump, diameter of the suction pipe, suction height, and inner pipe diameter, were used. The system performance was evaluated by investigating the relationship between the flow rates ($Q1$ and $Q2$), water head, and pressures $P1$ and $P2$. Two sets of high-pressure pumps capable of producing a combined $Q1$ of 10–11 $m^3/min$ were used. The system was tested at pump pressures ($P1$) of 0.8, 1.0, 1.3, and 1.5 MPa for the ejector's inner pipes of 200 and 250 mm. The associated suction flow ($Q2$) ranged from 7.9 to 12 $m^3/min$ and the measured pressures in the transport pipe ($P2$ and $P3$) varied from 0.08 to 0.18 MPa.

Evaluation of the dredging efficiency in Morotsuka reservoir was furnished by considering different suction pipe sizes, ejector depths, and applied flow rates ($Q1$) with and without air injection. As shown in Fig. 12, the flow rate ($Q2$) increases with the pump pressure, with generally a better response for 250-mm inner

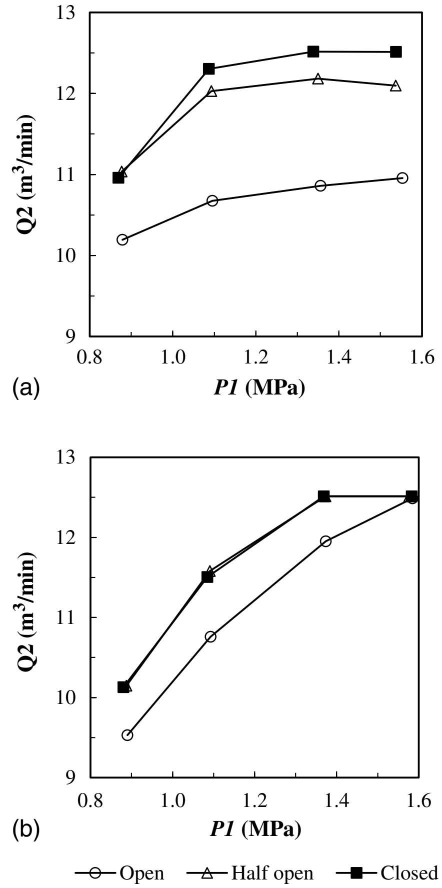


**Fig. 12.** Flow rate in suction pipe versus average pump pressure for the ejector inner pipe diameters of (a) 200 mm; and (b) 250 mm.

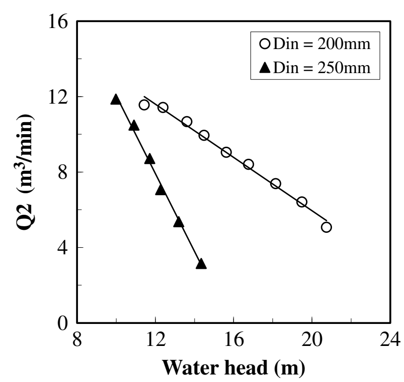


**Fig. 13.** Relation between suction flow rate ($Q_2$) and water head for different ejector inner diameters.

diameter than the 200-mm one. Plugging occurred in the transport pipeline when no air was injected into the system. The fully open air valve minimized plugging in the pipeline, but the flow rate was reduced. For the half-open valve and 200-mm inner diameter, there is no notable increase in flow rate with increasing $P1$ beyond 1.1 MPa. At the low $P1$ values, the flow associated with the 200-mm diameter was higher than that of the 250-mm one. Therefore, the former was perceived to be more efficient.

The relation between $Q2$ and water head of the system is shown in Fig. 13. The measured flow rate was almost the same for both pipe diameters at a water head of approximately 10 m. The 200-mm size outperformed the 250-mm diameter for larger water heads, up



J. Hydraul. Eng., 2021, 147(2): 04020098

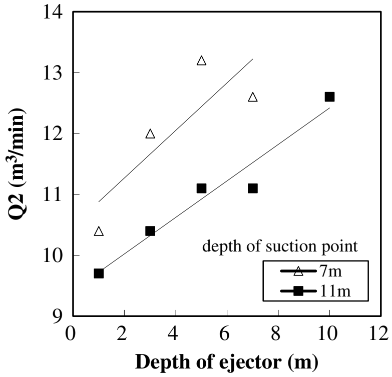


**Fig. 14.** Suction flow rate ($Q_2$) versus depth of ejector below water surface using a pump pressure of 1.86 MPa and a 15-m suction pipe.

to 21 m. The high head (pressure) associated with the use of the small inner pipe is obviously advantageous for the transportation ability of the system. The productivity was 120 $m^3/h$ for the 100-m-long transport line (Temmyo et al. 2013). However, for water heads less than 10 m and short transportation, the use of a large inner pipe is preferred for easier removal of large sediments.

The vertical position of the ejector pump with respect to the reservoir's bed can be adjusted using a lifting arm. The effect of the ejector's depth below the water surface on $Q2$ was investigated at a pump pressure of 1.86 MPa using a 15-m-long suction pipe (Fig. 14). Two suction depths were examined: 7 and 11 m. The relationship between the water depth and sediment transportation rate for all 58 cases was closely studied (Fig. S4). Similar to conventional hydraulic suction, locating the ejector pump deep under the water surface improved the suction efficiency of the system.

The excavated sediments from Oouchibaru reservoir were screened using 80- and 120-mm sieves to remove cobbles (Fig. S5). A screw crusher (Fig. S3) was used to break down the large driftwood into smaller pieces of approximately 150 mm prior to removal by EPDS. The crusher's shaft disintegrated the gravels entering in between the conical-shaped shaft and the lining plates in the shell. This allowed convenient removal of sediment sizes that could not be tackled using conventional submersible water pumps. Given the wide size range of sediments and driftwood, mechanical sieving was necessary to split the dredged sediments into two size fractions: smaller and larger than 100 mm. Oversized material was transported to the Oouchibaru reservoir for gravel capping. The maximum size of gravel removed by EPDS was around 150 mm. This highlights the need for modifying the EPDS to make it capable of removing coarser sediment larger than this size. The system, however, did not experience plugging or overdredging.

### *Sediment Transport and Relocation*

The relation between the pressure at the starting point of the transportation pipeline ($P2$) and the sediment transportation rate ($S$) is shown in Fig. 15(a) for the hopper-type EPDS. The observed transportation rates are linearly proportional to the pressure for three transportation lengths ($L_{tp}$) of 200, 600, and 1,000 m. The transportation rate decreased exponentially with the length [Fig. 15(b)]. This highlights the significant adverse effect of $L_{tp}$ on sediment transport efficiency. Combining the two factors, the sediment removal rate is linearly proportional to $P2/L_{tp}$ [Fig. 15(c)].

The air injected into the transportation pipeline was set at 36 and 54 $nm^3/min$ for the 600- and 1,000-m transport pipelines, respectively. For the initial water discharge of about 10 $m^3/min$, the ratio of the injected air into the system to the water discharge was

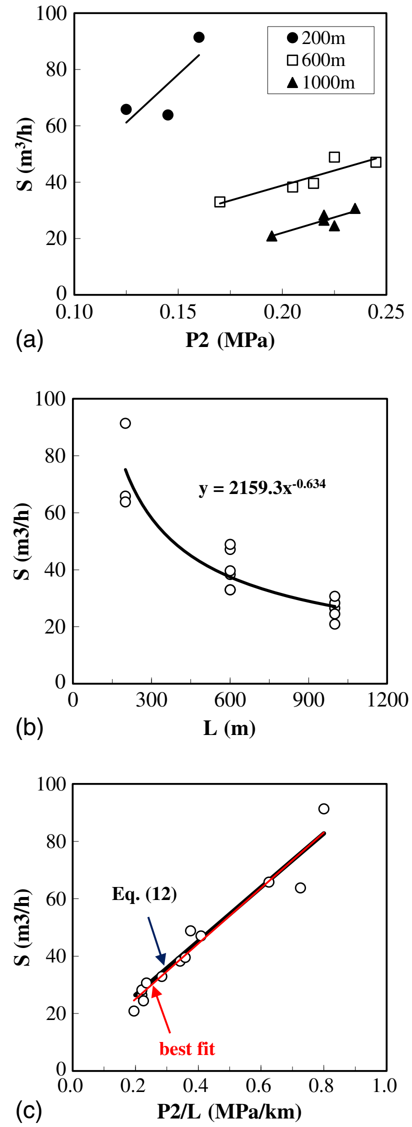


**Fig. 15.** Sediment transportation rate ($S$) using hopper-type EPDS for three transport pipe lengths (600, 800, 1,000 m) (a) versus $P2$; (b) versus $L$; and (c) versus $P2/L$. [$P2$ and $T$ = measured and estimated pressure at the starting point of the transport pipe; $L$ = transport pipe length; best fit line is $S = 96.8P2/L + 5.7$; Eq. (12): $S = 93.8T/L_{tp} + 7.71$].

approximately 3 to 6. At those air concentrations, the measured removal rates were approximately 30 and 50 $m^3/h$ for transport pipe lengths of 600 and 1,000 m, respectively. Based on the collected measurements, the maximum water head of the ejector pump is assumed to be proportional to the ratio of the nozzle to inner pipe sectional area ($D_n^2/D_i^2$) and the pump pressure. The estimated pressure at the starting point of the transportation pipeline ($T$) can therefore be expressed as follows:

$$T = (D_n^2/D_i^2)P1 + \alpha \tag{11}$$

where $D_n$ = nozzle diameter; $D_i$ = inner pipe diameter; and $\alpha$ = constant. The estimated pressure ($T$) is almost equal to the pressure $P1$ at $\alpha = 0.067$ [Fig. 15(c)]. This assumption holds for nozzle and inner pipe diameters ranging from 58 to 70 mm and from 200 to 250 mm, respectively. Within these ranges, the high-pressure pump delivers its energy proportional to $(D_n^2)/(D_i^2)$ ratio. The sediment transportation rate ($S$) can be related to the estimated $T/L_{tp}$ ratio as follows [Fig. 15(c)]:



J. Hydraul. Eng., 2021, 147(2): 04020098

$$S = 93.8T/L_{tp} + 7.71 \quad (12)$$

This relation between the estimated $S$ and $T/L_{tp}$ is supported by the best fit of the field measurements as shown in Fig. 15(c). Substituting Eq. (11) into (12) yields

$$S = 93.8/L_{tp}[(D_n^2/D_i^2)P1 + \alpha] + 7.71 \quad (13)$$

By simple manipulation of Eq. (13), the required pump pressure ($P1$) of the system can be accordingly estimated as

$$P1 = [(L_{tp}(S - 7.71))/93.8 - \alpha](D_i^2/D_n^2) \quad (14)$$

This equation can be used to estimate the pumping power needed to deliver a desired sediment removal rate ($S$) for a given set of geometrical configurations of the transport line ($D_i^2/D_n^2$ and $L_{tp}$). For example, if the targeted $S$ is 50 $m^3/h$ and a 1.0-km transportation pipe having a $D_i^2/D_n^2$ ratio of 8.1 (based on $D_i =$ 200 mm and $D_n = 70$ mm) is used, a 3.1-MPa pumping pressure is needed.

The dredged sediments were transported to closely investigate the performance and efficiency of the hopper-type dredger in the trial tests conducted in the Saigo reservoir. These sediments were relocated to a maximum transportation length of 1,000 m using a hopper attached to the ejector pump and a conveyor belt extended to the disposal area downstream of Oouchibaru reservoir. The grain size analysis of the fine portion of the dredged sediment showed that 88% of removed particles fell between 0.425 and 0.85 mm, with a mean size of 0.39 mm. The dredged material also included stone, gravel, branches, and debris. As a result of a relatively long suction pipeline, system blockage was encountered. The ejector pump was placed under the water surface to enhance suction. Thus, the distance between the ejector pump and the entrance of the suction pipeline (reservoir bed) can be adjusted to reduce the risk of sediment plugging. The EPDS was able to lift 3,500 $m^3$ of sediment from the reservoir's depths ranging from 3 to 15 m. The dredged sediments were subsequently relocated using a floating transportation pipeline to the disposal site, located 400 m upstream of the suction point.

### *Embracing Sustainable Sediment Management*

An integrated sediment management plan was implemented to ensure sustainable upgrading of the Mimi River basin. The EPDS system was utilized for sediment removal and relocation, and subsequent capping along the retrofitted dam sites (Turusaki et al. 2017). This solution has successfully restored and upgraded the Yamasubaru, Saigou, and Oouchibaru dams (Fig. S6).

Sluicing upstream of the Oouchibaru Dam was carried out in 2015. A total volume of 107,600 $m^3$ of gravel and sand capping was placed at the reservoir's bed before sluicing in order to combat possible high turbid water release downstream. Therefore, controlling and monitoring of turbidity were performed during construction. Turbid water generation was analyzed and estimated considering the material of gravel capping, method of execution, and diffusion properties of the turbid water outflow. The dredged material caps were placed in the reservoir by using the hopper-type EPDS.

It is expected that the turbidity level will decrease with the distance from the dredger and the reservoir bed. Fig. 16 displays the turbidity levels [in terms of the suspended sediment concentration (SSC)] at different times during dredging. The turbidity was monitored at different distances from the sediment injection point on both sides of the silt fence. Surface SSC values were the lowest for all turbidity measurements at different locations [Fig. 16(a)]. The values of SSC declined quickly with the distances from EPDS

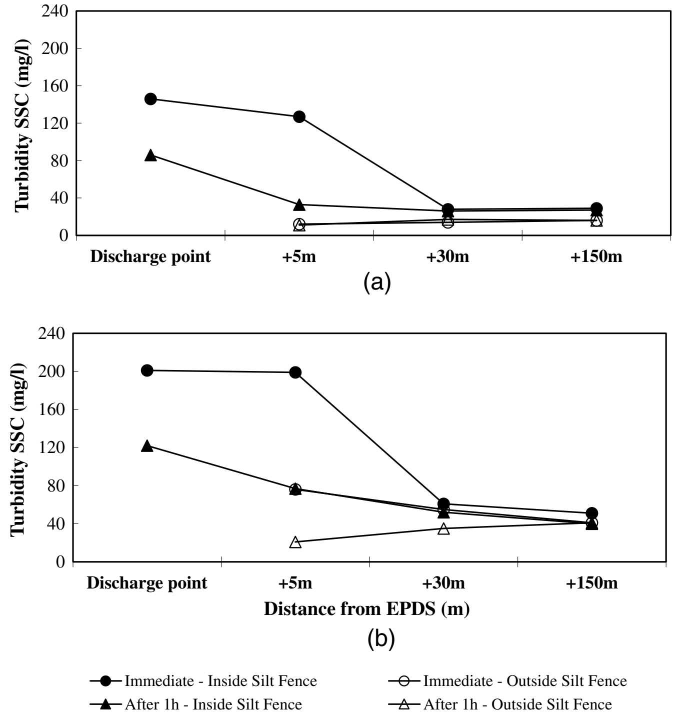


**Fig. 16.** Results of turbidity measurements in the vicinity of the EPDS injection points at different water depths: (a) surface; and (b) 5 m below the surface.

for all depths. A maximum turbidity of about 200 mg/L was measured at 5 m below the surface at the EPDS [Fig. 16(b)]. This value dropped below 50 mg/L at 150 m from the EPDS point. Furthermore, no plumes were observed behind EPDS for all full-scale pilot test. These observations collectively indicate an eco-friendly performance of the system and, ultimately, a minimal impact on the reservoir environment.

## System Optimization and Merits

The EPDS system provides a range of desirable characteristics and merits in sediment management programs. The eco-friendly performance of the system makes EPDS outshine all comparable dredging systems from the environmental standpoint. It works effectively as one unit up to a distance of 1,000 m from the suction point with no need for a booster. The production of the suction-type and hopper-type EPDS systems depends on the pump flow rate, ejector's depth and inner pipe diameter, and injected air concentration, which can be adjusted to maximize productivity. Therefore, the three types of field implementations (dredging, sediment transport with gravel capping, and sediment relocation) in Japanese reservoirs were quite helpful in testing the proposed optimal design of the system.

Field trials indicated that the maximum production for sandy and gravelly sediments can be achieved with air injections of 36 and 54 $nm^3/min$ for transport lengths of 600 and 1,000 m, respectively. The system allows uninterrupted (no plugging) sediment removal in water depths up to 20 m with a dredging capacity up to 70 and 35 $m^3/h$ in sandy and gravelly soils, respectively. The optimum dredging production rate occurs at a pumping capacity of about 10 $m^3/min$, using a 200-mm ejector inner pipe for suction lengths less than 8 m, and air concentrations of 40–60 $nm^3/min$. The maximum sediment removal using a hopper-type EPDS can be

**Table 2.** EPDS versus commercially available suction dredging systems

| System | Operating | Cost (million ¥)[a] | Dredging depth (m) | Productivity (day)[a] | Concerns |
|---|---|---|---|---|---|
| EPDS | High-pressure pump, jet water | 5.85 | >8 | 48 | — |
| Pump dredging | Sand pump with cutter | 7.43 | >20 | 51 | Turbidity and plugging |
| Hydrojet pump | Suction system | 2.65 | >50 | 70 | Blockage; fine sediment |
| Siphon dredging | Suction system | 2.87 | 1–6 | 39 | Clogging |
| Water injection | Injecting water into bed sediment | 3.75 | >14 | 40 | Environmental concern; infeasible in consolidated clay silt |
| Air lift pumps | Pressurized air injection | 4.35 | >50 | 30 | High water consumption; limited grain size |

[a]Per 10,000 $m^3$.



estimated from Eq. (13). In order to dredge various sediment types including hard clay and sandy sediments with greater depth (50–100 m), it is necessary to break down these materials using the auxiliary horizontal multiaxis cutter. The cutter can be replaced with a crusher to be adapted to various sediment conditions, which can include wood, clay, sand and rock.

The proposed EPDS and the commercially available hydraulic suction dredging systems are compared in Table 2. Generally, conventional suction dredgers yield 33 $m^3/h$ in sandy soils with no reported success in gravelly soils. For instance, the suction system by hydrojet pump has the lowest cost and provides the highest productivity. However, it is suitable only for fine sediment and for limited transportation length. Likewise, the siphon dredging has a limited dredging depth with a high potential of clogging in the transportation pipeline. The cost and production are highly variable because they are site specific, i.e., controlled by the transport distance to relocating sites, reservoir bathymetry, and types of bed sediments. In view of the limitations and pros and cons in each method, the cost and production comparison should be merely used as an indicator.

The injection of air into the EPDS system was instrumental for efficient dredging of fine- and medium-size deposits—the most commonly encountered sediments—using low suction power. This reduces the dredging cost and time and allows sediment transport over longer distances. The cost of the dredging for this system falls within the typical costs of the suction systems listed in Table 2. Compared to other systems, however, the productivity and cost effectiveness of the EPDS system are very attractive, particularly because of its low maintenance, limited environmental impact, and versatility.

## Conclusions

Continuous sediment deposition is a major recurring issue that hampers sustainable management of reservoirs. Due to the decreasing availability of suitable new dam sites, raising existing dams is always considered a practical solution to cope with the increasing water storage demand. However, this approach poses socioenvironmental threats to the habitat and public safety. To this end, it is imperative to adopt a holistic vision honoring sustainability and eco-friendly sediment management. The current study suggests a viable suction dredging technique for integrated sediment management of dam reservoirs. Combined with sediment bypassing, sediment removal using the proposed EPDS can reduce the magnitude and frequency of the required dredging. The three components (driving force, suction, and transportation) of the proposed EPDS work as an integrated unit for sediment dredging and transport in reservoirs of different sizes. The system has proven efficient dredging of coarse and fine sediments in both laboratory experimentation and field trials. Its simplicity and mobility allow versatile operations in remote or mountainous reservoirs. The EPDS system can be used to dredge and relocate sediments within a reservoir near dam sites and intake structures, with limited turbidity levels at the dredging and disposal points as well as during gravel capping operations.

## Data Availability Statement

All data, models, and code generated or used during the study appear in the published article and the supplemental material.

## Acknowledgments

The first two authors equally contributed to this manuscript. The experimental work of this research was conducted at Taiwan International University with collaboration of Ando Hazama Corporation and POJET co. The authors are indebted to the invaluable input and field trials performed by our industry partners. It is also inevitable to acknowledge Mr. Sandun Dassanayake, PhD candidate at Monash University Malaysia, for conducting some editorial tasks and providing additional references that supported our views and findings.

## Notation

*The following symbols are used in this paper:*

$A_p$ = cross-sectional area of transport pipeline ($m^2$);
$C_{ss}$ = concentrations of sediment removal in suction pipeline (%);
$C_{st}$ = concentrations of sediment removal in transport pipeline distance (%);
$D_i$ = diameter of inner pipe (mm);
$D_n$ = diameter of the nozzle (mm);
$d_s$ = sediment grain size (mm);
$D_{sp}$ = internal diameter of suction pipe (mm);
$D_{tp}$ = diameter of the transport pipeline (mm);
$E_{EPDS}$ = overall efficiency of system performance (%);
$H_{sp}$ = height of the suction pipeline (m);
$H_{suc}$ = height of the suction vertical pipeline (m);
J = total superficial velocity in the transport pipeline (m/s);
$J_A$ = superficial air velocity in the transport pipeline (m/s);
$J_W$ = superficial water velocity in the transport pipeline (m/s);
$L_{sp}$ = length of the suction pipeline (m);
$L_{tp}$ = length of transport pipeline (m);
$P_{pump}$ = pump discharge pressure (kPa);

$P1$ = initial pressure of water measured by pressure gauges located at the pump (kPa);
$P2$ = pressure measured at the beginning of the transport pipeline (kPa);
$P3$ = pressure measured at the end of the transport pipeline (kPa);
$Q_{air}$ = injected air concentration to the transport pipeline (nL/min);
$Q_{pump}$ = discharge of pump (L/min);
$Q_s$ = sediment discharge (transportation) rate for suction type (L/min);
$Q_{suc}$ = suction power [volume of water and sediment lifted during a specific time period (L/min) or water-sediment sucked from the reservoir];
$Q_{ws}$ = discharge of water-sediment through the transport pipeline (L/min);
$Q1$ = initial discharge measured by a flowmeter (L/min);
$Q2$ = flow rate in the suction pipeline measured by flowmeter (L/min);
$S$ = sediment transportation rate for hopper-type EPDS (volume of sediment placed on the bottom of the reservoir per hour);
$t_{ws}$ = time needed for suction and removal of water and sediment at the end of the transport pipe ($S$);
$V_s$ = volume of sediments initially placed in the storage tank (L);
$V_{ws}$ = volume of released water and sediment (L);
$\Delta x$ = distance between two piezometers/pressure probes;
$\rho_s$ = density of sediment (kg/m$^3$); and
$\rho_w$ = density of water (kg/m$^3$)

## Supplemental Materials

Figs. S1–S6 are available online in the ASCE Library (www.ascelibrary.org).

## References


Auel, C., S. A. Kantoush, and T. Sumi. 2016. "Positive effects of reservoir sedimentation management on reservoir life-examples from Japan." In *Proc., 84th Annual Meeting of ICOLD*. Johannesburg, South Africa: South African National Committee on Large Dams.

Basson, G. R., and A. Rooseboom. 1999. *Dealing with reservoir sedimentation: Dredging South Africa*. Pretoria, South Africa: Water Research Commission.

Bray, R. N., A. D. Bate, and J. M. Land. 1996. *Dredging: A handbook for engineers*. 2nd ed. Oxford, UK: Butterworth-Heinemann.

Bruk, S. 1985. *Methods of computing sedimentation in lakes and reservoirs: A contribution to the International Hydrological Programme, IHP-II Project A. 2.6.1. panel*. London: UNESCO.

Chaudhuri, B., A. Ghosh, B. Yadav, R. P. Dubey, P. Samadder, A. Ghosh, and S. Das. 2020. "Evaluation of dredging efficiency indices of TSHDs deployed in a navigational channel leading to Haldia Dock Complex." *J. Hydraul. Eng.* 2020 (Jun): 1–9. https://doi.org/10.1080/09715010.2020.1786738.

Dabirian, R., R. Mohan, O. Shoham, and G. Kouba. 2016a. "Critical sand deposition velocity for gas-liquid stratified flow in horizontal pipes." *J. Nat. Gas Sci. Eng.* 33 (Jul): 527–537. https://doi.org/10.1016/j.jngse.2016.05.008.

Dabirian, R., R. Mohan, O. Shoham, and G. Kouba. 2016b. "Solid-particles flow regimes in air/water stratified flow in a horizontal pipeline." *Oil Gas Facil.* 5 (6): 1–14. https://doi.org/10.2118/174960-PA.

Goharzadeh, A., P. Rodgers, and C. Touati. 2010. "Influence of gas-liquid two-phase intermittent flow on hydraulic sand dune migration in horizontal pipelines." *J. Fluids Eng.* 1327 (1): 71301. https://doi.org/10.1115/1.4001869.

Herbich, J. B. 2000. *Handbook of dredging engineering*. 2nd ed. New York: McGraw-Hill.

Kantoush, S. A., A. J. Schleiss, T. Sumi, and M. Murasaki. 2011. "LSPIV implementation for environmental flow in various laboratory and field cases." *J. Hydro-Environ. Res.* 5 (4): 263–276. https://doi.org/10.1016/j.jher.2011.07.002.

Kantoush, S. A., and T. Sumi. 2016. "The aging of Japan's dams: Innovative technologies for improving dams water and sediment management." In *Proc., 13th Int. Symp. on River Sedimentation ISRS*. Nottingham, UK: International Water Power & Dam Construction Magazine.

Kantoush, S. A., and T. Sumi. 2019. *Paradigm shift for sediment management*. Romford, UK: International Hydropower Association.

Kim, T. W., T. B. Aydin, E. Pereyra, and C. Sarica. 2018. "Detailed flow field measurements and analysis in highly viscous slug flow in horizontal pipes." *Int. J. Multiphase Flow* 106 (Sep): 75–94. https://doi.org/10.1016/j.ijmultiphaseflow.2018.05.005.

Leporini, M., B. Marchetti, F. Corvaro, G. di Giovine, F. Polonara, and A. Terenzi. 2018. "Sand transport in multiphase flow mixtures in a horizontal pipeline: An experimental investigation." *Petroleum* 52 (2): 161–170. https://doi.org/10.1016/j.petlm.2018.04.004.

Lewis, J. M., and R. E. Randall. 2015. "Prediction of minor loss coefficient at suction inlet of cutter suction dredge." *J. Dredging* 151 (1): 14–42.

Mandhane, J. M., G. A. Gregory, and K. Aziz. 1974. "A flow pattern map for gas—Liquid flow in horizontal pipes." *Int. J. Multiphase Flow* 1 (4): 537–553. https://doi.org/10.1016/0301-9322(74)90006-8.

Meshkati Shahmirzadi, M. E., T. Sumi, S. Kantoush, and T. Temmyo. 2012. "Influence of air injection on suction power and pressure gradient in dredger system." *J. Jpn. Soc. Civ. Eng.* 684 (1): 37–42. https://doi.org/10.2208/jscejhe.68.I_37.

Morris, G. L. 2020. "Classification of management alternatives to combat reservoir sedimentation." *Water* 12 (3): 861. https://doi.org/10.3390/w12030861.

Nakamura, Y., T. Okabe, T. Temmyo, T. Yamashita, M. Kaku, Y. Yamagami, O. Kuroki, T. Sumi, A. K. Sameh, and M. Mohammad. 2012. "A method of sediment transportation by special ejector pump system in the dam reservoir." In *Proc., Int. Symp. on Dams for Changing World*. Tokyo: Japan Commission on Large Dams.

Taitel, Y., and A. E. Dukler. 1976. "A model for predicting flow regime transitions in horizontal and near horizontal gas-liquid flow." *AIChE J.* 221 (1): 47–55. https://doi.org/10.1002/aic.690220105.

Temmyo, T., Y. Nakamura, Y. Yamagami, M. Kaku, T. Sumi, and M. E. Meshkati. 2013. "Sediment relocation trial by ejector pump dredger system (EPDS) in a dam reservoir." In *Proc., 12th Int. Symp. on River Sedimentation*. London: Taylor & Francis.

Tsurusaki, D., M. Kiyota, K. Asazaki, Y. Nakamura, T. Temmyo, M. Mizunuma, A. Mousa, S. A. Kantoush, and T. Sumi. 2017. "Gravel capping for turbidity control during sediment sluicing by the use of ejector pump system." In *Proc., 37th IAHR World Congress*. Beijing: International Association for Hydro-Environment Engineering and Research.

Turner, T. M. 1996. *Fundamentals of hydraulic dredging*. Reston, VA: ASCE.

Yamagami, Y. 2012. "Approaches for integrated sediment flow management at dams in the Mimikawa river basin." In *Proc., Int. Symp. on Dams for a Challenging World*. Tokyo: Japan Commission on Large Dams.